Efficacy Analysis of In Situ Synthesis of Nanogold via Copper/Iodonium/Amine/Gold System under a Visible Light

Jui-Teng Lin, Jacques Lalevée, Hsia-Wei Liu

polymers

MDPI

Article

Efficacy Analysis of In Situ Synthesis of Nanogold via Copper/Iodonium/Amine/Gold System under a Visible Light

Jui-Teng Lin [1], Jacques Lalevee [2] and Hsia-Wei Liu [3,*]

[1] New Photon Corp., 10F, No. 55, Sect. 3, Xinbei Blvd, Xinzhuang, New Taipei City 242062, Taiwan; jtlin55@gmail.com
[2] CNRS, IS2M UMR 7361, Université de Haute-Alsace, F-68100 Mulhouse, France; jacques.lalevee@uha.fr
[3] Department of Life Science, Fu Jen Catholic University, New Taipei City 242062, Taiwan
* Correspondence: 079336@gmail.com

Abstract: This article presents, for the first time, the kinetics and the general features of a photopolymerization system (under visible light), copper-complex/Iodonium/triethylamine/gold-chloride (orA/B/N/G), with initial concentrations of A_0, B_0, N_0 and G_0, based on the proposed mechanism of Tar et al. Analytic formulas were developed to explore the new features, including: (i) both free radical photopolymerization (FRP) efficacy and the production of nanogold (NG), which are proportional to the relative concentration ratios of $(A_0 + B_0 + N_0)/G_0$ and may be optimized for maximum efficacy; (ii) the two competing procedures of NG production and the efficacy of FRP, which can be tailored for an optimal system with nanogold in the polymer matrix; (iii) the FRP efficacy, which is contributed by three components given by the excited state of copper complex (T), and the radicals (R and S) produced by iodonium and amine, respectively; (iv) NG production, which is contributed by the coupling of T and radical (S) with gold ion; and (v) NG production, which has a transient state proportional to the light intensity and the concentration ratio A_0/G_0) + $(N_0/(K'M_0)$, but also a steady-state independent of the light intensity.

Keywords: polymerization kinetics; photoinitiator; free radical polymerization; copper complex; photoredox catalyst; nanogold particles

Citation: Lin, J.-T.; Lalevee, J.; Liu, H.-W. Efficacy Analysis of In Situ Synthesis of Nanogold via Copper/Iodonium/Amine/Gold System under a Visible Light. *Polymers* **2021**, *13*, 4013. https://doi.org/10.3390/polym13224013

Academic Editor: Gregory T. Russell

Received: 14 June 2021
Accepted: 15 November 2021
Published: 20 November 2021

1. Introduction

Light sources from UV (365 nm) to near-infrared (980 nm) have been used for photopolymerization reactions in many industrial and medical applications such as dental curing, microlithography, stereolithography, microelectronics, and holography [1,2]. A variety of photoresponsive materials such as conjugated polymers, organic dyes, and metal complexes have been reported for additive manufacturing (AM) and 4D bioprinting [3,4]. Both spatial and temporal controlled 3D processes were reported in systems using single and multiple wavelength lights [5,6]. We have previously reported various strategies for improved photopolymerization conversion, in which the efficacy enhancement is achieved by co-initiators and co-additives in multiple components systems [7–11].

Besides UV light photopolymerization, visible lights are also used for organic dyes photosensitizers [12,13], in which high extinction coefficients and their long-living excited states enable the photosensitizers to react efficiently with various additives in the photocurable resins. Cost effective and with long-living excited states, copper complexes have been used as a new polymerization approach to initiate the free radical polymerization (FRP) of acrylates or the free radical promoted cationic polymerization (CP) of epoxides, in which acetylacetonate radicals are produced by redox reaction [14–17]. Recently, using Coumarin as a dual function, photoinitiators for photo-oxidation and photo-reduction in visible light were reported [18–20]. The efficiency of the copper complex (G1) based photoinitiating systems of (G1/iodonium salt (Iod)/*N*-vinylcarbazole (NVK) was investigated by Mokbel et al. [16] for FRP and CP using light sources at 375, 395, and 405 nm.

More recently, our group reported the novel copper photoredox polymerization for in situ synthesis of metal nanoparticles (Tar et al. [21]) in which nanoparticles were embedded to the polymer matrix to enhance some particular properties of the parent matrix, called polymer nanocomposite. Metal complexes (zinc, ruthenium, iridium, and copper) have been used as photoinitiators for FRP and CP [16,17]. These photoinitiators have excellent photochemistry properties such as strong absorption in visible light, long steady-state excited state, and suitable redox potentials. Furthermore, they also provide dual function of the oxidation or the reduction cycle to produce reactive species—e.g., radicals, anions, or cations. Recently, copper complexes have been gaining more attention due to their comparatively low cost. In our previous work, a new copper complex based on a hydrazone ligand was proposed as a photocatalyst for the polymerization of ethylene glycol diacrylate simultaneously with the production of nanogold in a polymer network under exposure to an LED at 419 nm [21].

This article will present, for the first time, the kinetics and the general features of a photopolymerization system (under visible light), copper/iodonium/triethylamine/gold chloride, based on our proposed mechanism [21]. Analytic formulas will be developed to analyze and explore new features that have not been investigated in the measured data of Tar et al. [21].

2. Methods and Modeling Systems

The theoretical methods used in the present article include the following steps: (i) setup the photochemical kinetic equations based on the scheme proposed by Tar et al. [21]; (ii) solving the rate equations under the so-called quasi-steady-state conditions, and (iii) finding the efficacy of monomer conversion, which is defined by the time integral of the free radicals. Further details are shown as follows.

2.1. Photochemical Kinetics

A specific measured system was reported by Tar et al. [21] for their proposed kinetic (shown in Scheme 1) for a 3-component system of G1/Iod/amine, where G1 is a copper complex HLCuCl, amine is triethylamine (TEA), a reducing agents in the formation of gold nanoparticle inside the polymer matrix; and Iod is iodonium salt (oxidizing agent). The photoinitiating (PI) systems are mainly based on G1/TEA/Iodonium salt (0.05/1%/1% *w*/*w*) to the gold chloride ($HAuCl_4$), in which 4 wt% was added in a few drops of DMF, and the PI system was dissolved in ethylene glycol diacrylate (EGDA) at 93.95 wt%.

The reduction of $HAuCl_4$ occurs due to a transfer of electrons from the aminoalkyl radical, but also from the excited state of the copper complex (Cu*). The radical amine^0 produced from the coupling of Cu* and amine is able to abstract hydrogen to generate radicals, which reduces the tetrachloroaurate Au^{+3} to form Au^{+2}, which is then reduced to Au^{+1}, and further to Au^0, leading to the formation of nanogold (NG). The interaction of the G1, TEA, and gold chloride was very fast, (within 60 s) under a visible light at 419 nm. After 5 min under irradiation, the absorption of the complex and Au^{+3} entirely disappeared, having an increase in the absorption at the green (532 nm), which corresponds to the surface plasmon resonance (SPR) absorption [21–23]. The peak absorption (at 532 nm) of NG in a spherical shape moves toward near infrared (about 810 nm), if the NG is in a rod shape, with a length and width ratio of about 4.0 [24]. We note that the decomposition of the iodonium salt through an electron transfer and the production of aryl radical could also lead to NG. However, it is a secondary reaction, which is ignored in the present modeling.

We used the following short hand notations: A = copper complex, T = excited state, [HLCuCl]*, B = Iod; N is triethylamine (TEA), R = $[HLCuCl]^{+*}$, G = $Au^{+3,}$, G′ = Au^{+2} or Au^{+1}. The monomer (M) is EGDA (for FRP conversion). The associated Chart for Scheme 1 is shown in Figure 1 (only the key components are shown). As shown by Figure 1, a 3-initiator system (A/B/N) defined by the ground state of initiator A, which is excited to its first-excited state, and a triplet excited state (T), having a quantum yield (q). The triplet state T interacts with initiator [B], leading to regenerating A and producing a radical R. It

can also interact with N to produce another radical S. Both radicals (R and S) can interact with the monomer (M) for FRP. Furthermore, T and R can interact with the gold (G) to produce exited-gold (G'), which further couples with T and S, leading to the formation of NG in the polymer matrix. We note that Figure 1 is more general than that of Scheme 1, because it can be used in a general 3-component system, A/B/N, having a various initiator (A), or additives (B and N) and in various metal chlorid (such as gold and silver). The present article focuses on the feature of NG production and limits to FRP. The general case with both FRP and CP has been presented elsewhere [19,20].

Cu + (light) -> Cu* (excited state) (R1)

Cu* + Ar2I(+) -> Cu(+) + Ar° + ArI (R2)

Cu* + amine -> Cu(-) + amine(°+) (R3)

amine(°+) -> amine° + H(+) (R4)

Cu* + Au(3+) -> Cu(+) + Au(2+) (R5)

Cu* + Au(2+) -> Cu(+) + Au(1+) (R6)

Cu* + Au(1+) -> Cu(+) + Au(0) (R7)

amine° + Au(3+) -> amine(+) + Au(2+) (R8)

amine° + Au(2+) -> amine(+) + Au(1+) (R9)

amine° + Au(1+) -> amine(+) + Au(0) (R10)

Scheme 1. A proposed kinetics for a 3-component system of G1/Iod/amine in gold chloride ($HAuCl_4$) solution, where G1 is the copper complex (HLCuCl), having an excited state Cu*, which couples with iodonium salt, $Ar_2I(+)$, and amine to produce radicals, (Ar^0 and $amine^0$) which lead to FRP. Both Cu* and $amine^0$ can couple with Au(3+) to form Au(2+), then Au(1+), leading to Au(0) and the nanogold [21].

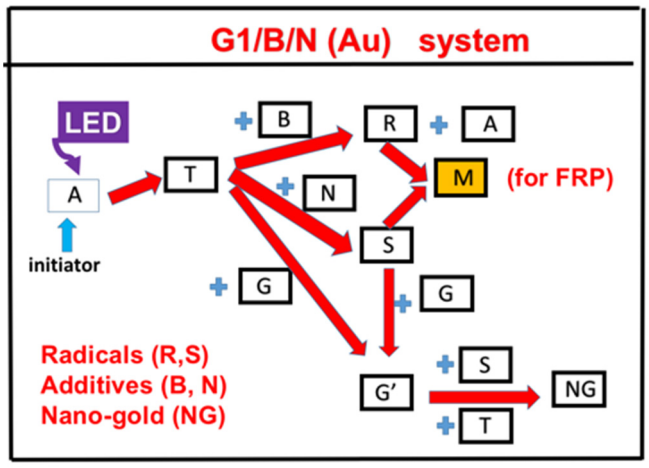

Figure 1. The schematics of a 3-component system, (A/B/N), where A is the ground state of initiator-A, having an excited triplet state T, which interacts with additives [B] and [N} to produce radicals R and S, which can interact with the monomer (for FRP), or interact with the gold (G, or Au^{+3}) to produce exited-gold (G', or Au^{+2} and Au^{+1}), which then further couples with T and S, leading to the formation of nanogold (NG, or Au^0) in the polymer matrix.

2.2. The Rate Equations

The kinetic equations for the concentration of each component of the 3-components (A/B/N) system (shown in Figure 1 and Scheme 1) are constructed as follows [19,25–27].

$$\frac{d[A]}{dt} = -\,bI[A](1 - R_E), \tag{1}$$

$$\frac{d[B]}{dt} = -k_1 T[B], \tag{2}$$

$$\frac{dN}{dt} = -k_2 T[N], \tag{3}$$

$$\frac{dT}{dt} = bI[A] - (k_7 + k_1[B] + k_2[N] + k_3 G + k_5 G' + kM)T, \tag{4}$$

$$\frac{dR}{dt} = k_1[B]T - \left(k'R + k''S + KM\right)R, \tag{5}$$

$$\frac{dS}{dt} = k_2[N]T - \left(\, k_4 G + k_6 G' + k''R + K'M\right)S, \tag{6}$$

$$\frac{dG}{dt} = -(k_3 T \;+\; k_4 S)G, \tag{7}$$

$$\frac{dG'}{dt} = (k_3 T \;+\; k_4 S)G - (k_5 T + k_6 S)G', \tag{8}$$

In Equation (1) R_E is the regeneration (REG) term of of the initiator, [A], given by $R_E = g(k_7 + k_1[B])$, with $g = k_7 + k_1[B] + k_2[N] + k_3 G$. $b = 83.6a'wq$, where w is the light wavelength (in cm) and q is the triplet state T quantum yield; a' is the mole absorption coefficient, in (1/mM/%) and I (z, t) is the light intensity, in mW/cm^2. All the rate constants are defined previously [25,27] and they are related by the coupling terms. For examples, k_j (with j = 1,2,3) are for the couplings of T and [B], [N], and G, respectively; K is for the coupling radicals R with monomer M (for FRP). In the above kinetics, we include the bimolecular termination [25] given by k'RR coupling in Equation (5), but for analytic formulas, we will keep only the unimolecular coupling term, KM, for FRP.

The monomer conversions for FRP and generation of NG are given by

$$\frac{dM}{dt} = -\left(kT + KR + K'S\right)M, \tag{9}$$

$$\frac{d[NG]}{dt} = (k_5 T + k_6 S)G', \tag{10}$$

For comprehensive modeling, we will use the so-called quasi-steady state assumption [25–27]. The lifetime of the singlet and triplet states of photosensitizer, the triplet state (T), and the radicals (R, S and G') is short, since they either decay or react with cellular matrix immediately after they are created. Thus, one may set $dT/dt = dR/dt = dS/dt = dG'/dt = 0$, which gives the quasi-steady-state solutions: $T = bIg[A]$, $R = k_1 bIgg'[A]\,[B])$, $S = k_2 bIgg''[A]\,[N])$, $G' = (k_3 T + k_4 S)/(k_5 T + k_6 S)$; with $g = 1/(k_7 + k_1[B] + k_2[N] + k_3 G + k_5 G' + kM)$, $g' = 1/(k''S + KM)$, $g'' = 1/(k_4 G + k_6 G' + k''R + K'M)$.

Under the above quasi-steady-state solutions, we obtain the simplified equations as follows.

$$\frac{d[A]}{dt} = -\,bI[A](1 - R_E), \tag{11}$$

$$\frac{d[B]}{dt} = -k_1 bIg[A][B]\,, \tag{12}$$

$$\frac{dN}{dt} = -k_2 bIg[A][N], \tag{13}$$

$$\frac{dG}{dt} = -bIg[A](k_3 + k_2 g''[N])G. \quad (14)$$

The monomer conversions for FRP and generation of NG are given by [27]

$$\frac{dM}{dt} = -bIg[A]\left(k + k_1 Kg'[B] + k_2 K'g''[N]\right)M, \quad (15)$$

$$\frac{d[NG]}{dt} = bIg[A](k_5 + k_6 k_2 g''[N]) \quad (16)$$

3. Results and Discussion

A full numerical simulation is required for the solutions of Equations (11)–(16), which will be presented elsewhere. We will focus on comprehensive analysis for special features and the key factors for efficient producing of NG related to the measured data of Tar et al. [22], based on the analytic formulas.

3.1. Analytic Results

Analytic formulas need assumption of strong coupling of T and [B], and KM >> k″S, K′M >> k_4G such that g = 1/(k_3G), g′ = 1/(KM), and g″ = 1/(K′M). In addition, R_E is taken as a mean reduction factor (f′), such that (1–R_E) = f′ = [1 − k_2N_0/(k_3G_0)] is time independent, having a value of f′ = 0.5 to 1.0. The first-order solutions of Equation (11) to (15) are found: [A] = A_0 exp(–dt); with d = f′bI; [B] = B_0 exp(-H), with H(t) = DE(t), with E(t) = [1 – exp(–dt)]/d]; [N] = N_0 exp(–H′), H′ = D′(k_2/k_1)D, with D = (k_1/k_3)d(A_0/G_0). Also G(t) = G_0 – (k_1/k_3)dt; G′ = (k_3/k_5)[1 + k_4S/T] = (k_3/k_5)[1 + k_4[N]/(KM), for k_5T >> k_6S. Using these approximated solutions, Equations (15) and (16) become

$$\frac{dM}{dt} = -kF(t)M - F(k_1[B\} + k_2[N]), \quad (17)$$

$$\frac{d[NG]}{dt} = F(t)\left(k_5 + \frac{k_6 k_2[N]}{K'M}\right)G', \quad (18)$$

where F′(t) = bI[A](k_3G).

Solving Equation (17), we obtain the first-order solution, with G(t) = G_0, and G′ = (k_3/k_5).

$$M = M_0 \exp[-P(t)] + Ho(t), \quad (19)$$

where P(t) = Q [1− exp(−dt)]/d]; with Q = (k/k_3)bI(A_0/G_0); and Ho(t) is a complex second order term proportional to bIA_0(k_1B_0 + k_2N_0/B_0)/G_0. We note that P(t) has a transient state value P = Qt, and steady-state value, P = Q/d, which is independent of the light intensity.

The production of nanogold, [NG], is given by the solution of Equation (18),

$$[NG](t) = D'[E(t) + Q'E'(t)], \quad (20)$$

where Q′ = (k_6k_2/k_3)(N_0/(K′M_0), E(t) = [1– exp(–dt)]/d]; E′(t) = [1– exp(–d′t)]/d′]; D′ = bI(A_0/G_0); d′ = d + (k_1/k_3)D, D = (k_1/k_3)d(A_0/G_0). We note that [NG](t) has a transient state value [NG] = D′(1 + Q′t); and steady-state value, [NG] = D′(1/d + Q′/d′), which is independent to the light intensity.

3.2. General Features and New Findings

As shown by Equations (17)–(20), the following significant features of the A/B/N/Gold, or Cu/Iod/Amine/Gold, system are summarized as follows (referred also to Scheme 1 and Figure 1).

(i) The additive [B], or Iod (an oxidizing agent) interacts with copper excited state (T, or Cu*) to produce radical (R) and also to regenerate the initiator, [A] (or Cu), shown by R_E = g(k_7 + k_1[B]) term in Equation (11).

(ii) The additive, [N] (or amine), has dual functions: interacting with T to produce additional radical (S, or amine^0) which leads to FRP; and coupled with G, or Au(3+), to form Au(2+), then G', or Au(1+), leading to Au(0) and the nanogold (NG).

(iii) Equations (9) and (17) show that the FRP is contributed by three components: from the coupling of monomer (M) with T, R, and S. The conversion efficacy is proportional to bI(A_0+ k_1 B_0 + k_2N_0)/(k_3G_0). which is an increasing function of the absorption coefficient (b) and light intensity (I), and the concentration ratios of (A_0 + B_0 + N_0)G_0.

(iv) Equations (10) and (18) show that the production of NG is contributed by two components given by the coupling term of (k_5T + k_6S)G' shown by Equation (10). In addition, as shown by Equation (20), [NG](t) has a transient state value [NG] = D'(1 + Q')t, which is an increasing function of bI[(A_0/G_0) + (N_0/(K'M_0); and the steady-state value, [NG] = D'(1/d + Q'/d'), which is independent to the light intensity.

Besides the above-described features, our modeling has explored the follow new findings, which are not observed in the experiment of Tar et al. [21].

(a) Both FRP efficacy and the production of NG are proportional to the relative concentration ratios of (A_0 + B_0 + N_0)/G_0, rather than the individual concentrations. Therefore, the photoinitiating system reported by Tar et al. [21] based on G1/TEA/Iodonium, having (0.05/1%/1% wt) and 4 wt% of gold chlorid (G_0, or $HAuCl_4$), is not optimized. Our modeling predicts that lower initial gold chlorid (G_0) and/or larger (A_0 + B_0 + N_0), leads to a higher ratio of (A_0 + B_0 + N_0)/G_0, and therefore higher FRP and larger production of NG. It seems that Tar et al. [21] have used a too high concentration of gold, but too low G1 concentration. In addition, our formula of Equation (19) predicts an optimal value of the concentration ratio (A_0 + B_0 + N_0)/G_0, as also predicted by our previous modeling in other systems by Lin et al. [19,28].

(b) We note that [B] plays no role in the production of NG under the first-order solution, but plays a minor role reducing the NG production, as shown by our second-order factor g = (1 − k_1[B]/G − k_2[N]/G)/(k_3G). Furthermore, there is a reduction effect in the FRP efficacy due to the production of NG caused by the reduction of excited state (T) when it couples with gold, Au(+3). On the other hand, higher FRP (or larger K'M term) also reduces the efficacy of NG production, as shown by the factor Q' = (k_6k_2/k_3)(N_0/(K'M_0) in Equation (20). Therefore, one may tailor the ratio of (A_0, B_0, N_0)/G_0 to achieve maximum NG production, but also the strength of polymer matrix (or higher FRP), which is a competing procedure of NG production.t

4. Conclusions

Analytic formulas are developed to explore the kinetics of a G1/ Iodonium/ TEA/gold chlorid (or A/B/N/G) system. We found that the FRP efficacy is governed by the coupling of the excited state of copper complex (T) with the radicals (R and S) produced by iodomium and amine, respectively. NG production has a transient state proportional to the light intensity, whereas it is independent to the light intensity at steady-state. The competing between NG production and efficacy of FRP can be tailored by the relative concentration ratios of (A_0 + B_0 + N_0)/G_0, which has an optimal value with nanogold in the polymer matrix.

Author Contributions: Conceptualization, J.-T.L., H.-W.L., and J.L.; methodology, H.-W.L. and J.-T.L.; data curation, J.-T.L. and H.-W.L.; formal analysis, H.-W.L. and J.-T.L.; funding acquisition, H.-W.L.; investigation, H.-W.L. and J.-T.L.; project administration, H.-W.L.; software, J.-T.L.; supervision, J.-T.L. and H.-W.L.; validation, J.-T.L., H.-W.L., and J.L.; writing—original draft, J.-T.L.; writing—review and editing, J.-T.L., and H.-W.L. All authors have read and agreed to the published version of the manuscript.

Funding: J.L. is acknowledged s The Agence Nationale de la Recherche (ANR agency) for its financial support through the NoPerox grant. H.-W.L. is thankful for the financial support from the Ministry of Science and Technology (grant number 108-2221-E-030-010-MY2).

Institutional Review Board Statement: Not applicable.

Informed Consent Statement: Not applicable.

Data Availability Statement: The data presented in this study are available on request from the corresponding author.

Acknowledgments: J.-T.L. is thankful for the internal grant from New Photon Corp.

Conflicts of Interest: J.-T.L. is the CEO of New Photon Corp.

References

1. Fouassier, J.P.; Lalevée, J. *Photoinitiators for Polymer Synthesis: Scope, Reactivity and Efficiency*; Wiley-VCH Verlag GmbH & Co. KGaA: Weinheim, Germany, 2012.
2. Yagci, Y.; Jockusch, S.; Turro, N.J. Photoinitiated Polymerization: Advances, Challenges, and Opportunities. *Macromolecules* **2010**, *43*, 6245–6260. [CrossRef]
3. Ligon, S.C.; Liska, R.; Stampfl, J.; Gurr, M.; Mülhaupt, R. Polymers for 3D Printing and Customized Additive Manufacturing. *Chem. Rev.* **2017**, *117*, 10212–10290. [CrossRef]
4. Kelly, B.E.; Bhattacharya, I.; Heidari, H.; Shusteff, M.; Spadaccini, C.M.; Taylor, H.K. Volumetric additive manufacturing via tomographic reconstruction. *Science* **2019**, *363*, 1075–1079. [CrossRef] [PubMed]
5. de Beer, M.P.; van der Laan, H.L.; Cole, M.A.; Whelan, R.J.; Burns, M.A.; Scott, T.F. Rapid, continuous additive manufacturing by volumetric polymerization inhibition patterning. *Sci. Adv.* **2019**, *5*, eaau8723. [CrossRef] [PubMed]
6. Van Der Laan, H.L.; Burns, M.A.; Scott, T.F. Volumetric Photopolymerization Confinement through Dual-Wavelength Photoinitiation and Photoinhibition. *ACS Macro Lett.* **2019**, *8*, 899–904. [CrossRef]
7. Lin, J.T.; Chen, K.T.; Cheng, D.C.; Liu, H.W. Dual-wavelength (UV and Blue) controlled photopolymerization confinement for 3D-printing: Modeling and analysis of measurements. *Polymers* **2019**, *11*, 1819. [CrossRef] [PubMed]
8. Lin, J.T.; Liu, H.W.; Chen, K.T.; Cheng, D.C. 3-wavelength (UV, blue, red) controlled photopolymerization: Improved conversion and confinement in 3D-printing. *IEEE Access* **2020**, *8*, 49353–49362. [CrossRef]
9. Chiu, Y.C.; Cheng, D.C.; Lin, J.T.; Chen, K.T.; Liu, H.W. Dual-function enhancer for near-infrared photopolymerization: Kinetic modeling for improved efficacy by suppressed oxygen inhibition. *IEEE Access* **2020**, *8*, 83465–83471. [CrossRef]
10. Lin, J.T.; Chen, K.T.; Cheng, D.C.; Liu, H.W. Enhancing blue-light-initiated photopolymerization in a three-component system: Kinetic and modeling of conversion strategies. *J. Polym. Res.* **2021**, *28*, 2. [CrossRef]
11. Lin, J.; Cheng, D.; Chen, K.; Chiu, Y.; Liu, H. Enhancing UV Photopolymerization by a Red-light Preirradiation: Kinetics and Modeling Strategies for Reduced Oxygen Inhibition. *J. Appl. Polym. Sci.* **2020**, *58*, 683–691. [CrossRef]
12. Dietlin, C.; Schweizer, S.; Xiao, P.; Zhang, J.; Morlet-Savary, F.; Graff, B.; Fouassier, J.-P.; Lalevée, J. Photopolymerization upon LEDs: New photoinitiating systems and strategies. *Polym. Chem.* **2015**, *6*, 3895–3912. [CrossRef]
13. Pigot, C.; Noirbent, G.; Brunel, D.; Dumur, F. Recent advances on push–pull organic dyes as visible light photoinitiators of polymerization. *Eur. Polym. J.* **2020**, *133*, 109797. [CrossRef]
14. Garra, P.; Dietlin, C.; Morlet-Savary, F.; Dumur, F.; Gigmes, D.; Fouassier, J.-P.; Lalevée, J. Redox two-component initiated free radical and cationic polymerizations: Concepts, reactions and applications. *Prog. Polym. Sci.* **2019**, *94*, 33–56. [CrossRef]
15. Noirbent, G.; Dumur, F. Recent Advances on Copper Complexes as Visible Light Photoinitiators and (Photo) Redox Initiators of Polymerization. *Catalysts* **2020**, *10*, 953. [CrossRef]
16. Mokbel, H.; Anderson, D.; Plenderleith, R.; Dietlin, C.; Morlet-Savary, F.; Dumur, F.; Gigmes, D.; Fouassier, J.; Lalevée, J. Simultaneous initiation of radical and cationic polymerization reactions using the "G1" copper complex as photoredox catalyst: Applications of free radical/cationic hybrid photopolymerization in the composites and 3D printing fields. *Prog. Org. Coat.* **2019**, *132*, 50–61. [CrossRef]
17. Rahal, M.; Mokbel, H.; Graff, B.; Toufaily, J.; Hamieh, T.; Dumur, F.; Lalevée, J. Mono vs. Difunctional Coumarin as Photoinitiators in Photocomposite Synthesis and 3D Printing. *Catalyst* **2020**, *10*, 1202. [CrossRef]
18. Rahal, M.; Graff, B.; Toufaily, J.; Hamieh, T.; Noirbent, G.; Gigmes, D.; Dumur, F.; Lalevée, J. 3-Carboxylic Acid and Formyl-Derived Coumarins as Photoinitiators in Photo-Oxidation or Photo-Reduction Processes for Photopolymerization upon Visible Light: Photocomposite Synthesis and 3D Printing Applications. *Molecules* **2021**, *26*, 1753. [CrossRef] [PubMed]
19. Lin, J.-T.; Lalevee, J.; Cheng, D.-C. A Critical Review for Synergic Kinetics and Strategies for Enhanced Photopolymerizations for 3D-Printing and Additive Manufacturing. *Polymers* **2021**, *13*, 2325. [CrossRef] [PubMed]
20. Abdallah, M.; Hijazi, A.; Lin, J.-T.; Graff, B.; Dumur, F.; Lalevée, J. Coumarin Derivatives as Photoinitiators in Photo-Oxidation and Photo-Reduction Processes and a Kinetic Model for Simulations of the Associated Polymerization Profiles. *ACS Appl. Polym. Mater.* **2020**, *2*, 2769–2780. [CrossRef]
21. Tar, H.; Kashar, T.I.; Kouki, N.; Aldawas, R.; Graff, B.; Lalevée, J. Novel Copper Photoredox Catalysts for Polymerization: An In Situ Synthesis of Metal Nanoparticles. *Polymers* **2020**, *12*, 2293. [CrossRef]
22. Lin, J.-T. Modeling the scaling law of surface plasmon resonance in gold spherical nanoshells. *J. Nanophotonics* **2010**, *4*, 049507. [CrossRef]
23. Lin, J.-T. Nonlinear optical theory and figure of merit of surface plasmon resonance of gold nanorods. *J. Nanophotonics* **2011**, *5*, 051506. [CrossRef]
24. Lin, J.T. Scaling law and figure of merit of biosensor using gold nanoshells. *J. Nanophotonics* **2010**, *4*, 049507. [CrossRef]

25. Lin, J.-T.; Cheng, D.-C. Modeling the efficacy profiles of UV-light activated corneal collagen crosslinking. *PLoS ONE* **2017**, *12*, e0175002. [CrossRef]
26. Lin, J.-T. Kinetics of Enhancement for Corneal Cross-linking: Proposed Model for a Two-initiator System. *Ophthalmol. Res. Int. J.* **2019**, *10*, 1–6. [CrossRef]
27. Lin, J.-T.; Liu, H.-W.; Chen, K.-T.; Cheng, D.-C. Modeling the Kinetics, Curing Depth, and Efficacy of Radical-Mediated Photopolymerization: The Role of Oxygen Inhibition, Viscosity, and Dynamic Light Intensity. *Front. Chem.* **2019**, *7*. [CrossRef]
28. Lin, J.-T.; Liu, H.-W.; Chen, K.-T.; Cheng, D.-C. Modeling the Optimal Conditions for Improved Efficacy and Crosslink Depth of Photo-Initiated Polymerization. *Polymers* **2019**, *11*, 217. [CrossRef] [PubMed]